Spin Solar Cell Phenomenon on Single Molecule Magnet(SMM) Impacted CoFeB based Magnetic Tunnel Junctions

Marzieh Savadkoohi [1,2], Daniel Gopman[2], Pius Suh[1], Carlos Rojas-Dotti,[3] José Martínez-Lillo,*[3] Pawan Tyagi*[1]
Mechanical Engineering, University of the District of Columbia, 4200 Connecticut Avenue, Washington DC, 20008, USA[1],
Materials Science and Engineering Division, National Institute of Standards and Technology, 100 Bureau Drive, Gaithersburg, MD 20899, USA [2]
Departament de Química Inorgànica / Instituto de Ciencia Molecular (ICMol), University of Valencia, Blasco Ibanez Boulevard, Valencia 46010, Spain[3]
Corresponding Author Emails: ptyagi@udc.edu

ABSTRACT: The single-molecule magnet (SMM) is demonstrated here to transform conventional magnetic tunnel junctions (MTJ), a memory device used in present-day computers, into solar cells. For the first time, we demonstrated an electronic spin-dependent solar cell effect on an SMM-transformed MTJ under illumination from unpolarized white light. We patterned cross-junction-shaped devices forming a CoFeB/MgO/CoFeB-based MTJ. The MgO barrier thickness at the intersection between the two exposed junction edges was less than the SMM extent, which enabled the SMM molecules to serve as channels to conduct spin-dependent transport. The SMM channels yielded a region of long-range magnetic ordering around these engineered molecular junctions. Our SMM possessed a hexanuclear $[Mn_6(\mu_3\text{-}O)_2(H_2N\text{-}sao)_6(6\text{-}atha)_2(EtOH)_6]$ [H_2N-saoH = salicylamidoxime, 6-atha = 6-acetylthiohexanoate] complex and thiols end groups to form bonds with metal films. SMM-doped MTJs were shown to exhibit a solar cell effect and yielded ≈ 80 mV open-circuit voltage and ≈ 10 mA/cm^2 saturation current density under illumination from one sun equivalent radiation dose. A room temperature Kelvin Probe AFM (KPAFM) study provided direct evidence that the SMM transformed the electronic properties of the MTJ's electrodes over a lateral area in excess of several thousand times larger in extent than the area spanned by the molecular junctions themselves. The decisive factor in observing this spin photovoltaic effect is the formation of SMM spin channels between the two different ferromagnetic electrodes, which in turn is able to catalyze the long-range transformation in each electrode around the junction area.

Keywords: Spin; SMM; MTJ; Solar Cell; photovoltaic effect

INTRODUCTION:

Spintronics is the utilization of spins degree of freedom to produce novel transport behavior for wide applications ranging from quantum computing and neuromorphic computing to high storage density and non-volatile Random-Access Memories (MRAMs) [1]. New technological applications may be soon forthcoming with recent discoveries of overlap between solar cell technologies and spintronics[2-4]. Like conventional electronics for many decades, the solar cell and photovoltaics applied discipline have been primarily focused on electrical transport and electronic materials properties, in the limit where electron spin is neglected in understanding solar electricity generation. In the last two decades, researchers have made advances in understanding spin-dependent solar cell behavior [2-4]. Spin has been demonstrated to play a direct role in the light absorption mechanism and in the establishment of an intrinsic spin electrochemical potential to drive charge through a given material. Researchers have used different approaches to study spin photovoltaic effects to improve solar cells' yield and efficiency. Conventional charge-based p-n junctions [5-7], quantum wires and nanoscale channels, and metal/nonmagnetic semiconductor systems [8-11] are a variety of platforms used for observing spin photovoltaic or spin solar cell effect [2,12]. These different approaches bring a variety of mechanisms to evaluate the role of electron spins in spin-dependent light absorption and photovoltaic effect. However, further advances are needed

beyond these initial observations to realize substantially larger magnitude spin-dependent photovoltaic effects.

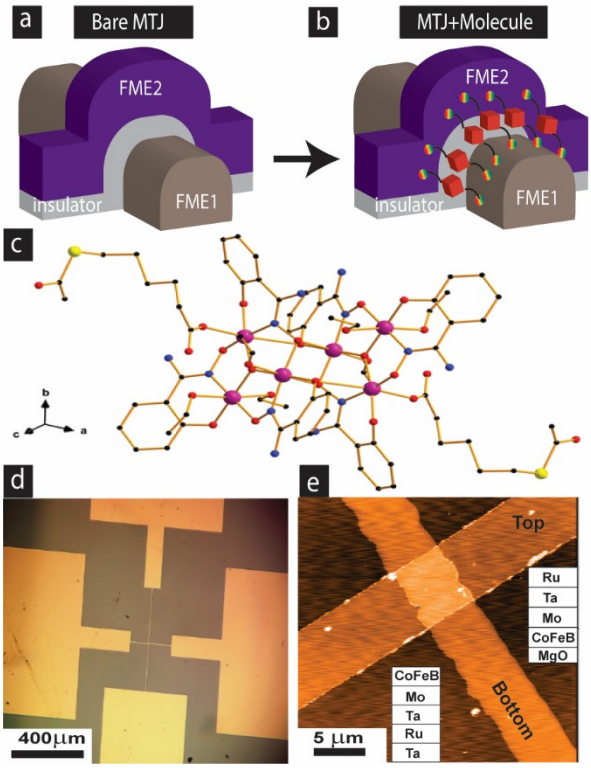

Figure 1: MTJMSD configuration (a) Bare and, (b) After molecular treatment. (c) Single-Molecule Magnet (SMM) structure (d) Optical microscope image of MTJMSC's cross junction (e) AFM scan of MTJMSD's cross junction

Recently, molecular spintronics devices have been reported to exhibit solar cell phenomena under regular unpolarized light radiation, particularly in a prototype platform comprising a C_{60} molecule and ferromagnetic interfaces [13]. In our prior work, we demonstrated the spin-dependent solar cell effect on magnetic tunnel junction (MTJ) based molecular spintronics device (MTJMSD) architecture [14]. For the first time, we observed that paramagnetic molecules transformed ferromagnetic NiFe electrodes into semiconducting material that responded to light. Prior MTJMSD utilized NiFe/AlOx/NiFe/Co MTJ structure[15] and S=6 cyanide-bridged octanuclear (Fe4Ni4II)-Ni-III complex paramagnetic molecules[16]. In this case, paramagnetic molecular channels themselves did not absorb light. However, they transformed the ferromagnetic electrodes (FME) in such a way the MTJ started showing p-n junction diode-like transport characteristics [14]. However, this study raised several key questions, including whether the MTJMSD-based solar cell phenomenon is limited to the combination of MTJ and (Fe4Ni4II)-Ni-III complex molecules [16]. Another question was about the effect of dissimilar ferromagnetic electrodes comprising the MTJ. It is noteworthy that we previously did not observe spin photovoltaic effects in MTJs with identical ferromagnetic electrodes [17]. We hypothesized that significant dissimilar ferromagnetic electrodes are necessary to see molecule-based spin photovoltaic effect. In this paper, we investigate CoFeB and MgO-based MTJ. Here, we report the observation of the solar cell effect on the MTJMSD involving MTJ with regularly utilized thin film stack configuration in MTJ based memory devices. This paper also reports intriguing observation of large-scale ordering produced by the SMM molecular channels on MTJ ferromagnetic electrodes.

EXPERIMENTAL DETAILS: We formed MTJMSD devices by applying SMMs as molecular channel bridging between the ferromagnetic electrodes of the patterned MTJ cross-junction devices. Patterned MTJ were deposited using a combination of direct current and radio frequency magnetron sputter deposition [17] (Fig. 1c). This custom-designed SMM molecule (Fig. 1c) was successfully utilized in forming MTJMSD. We have used cross-junction-shaped isolated MTJs to minimize interference from neighboring devices (Fig. 1d). To observe the photovoltaic effect, an MTJ was deposited with the following layer stacking structure: Ta(5 nm)/Ru(8 nm)/Ta(5 nm)/Mo(1 nm)/CoFeB(6 nm)/MgO(2 nm)/CoFeB(4 nm)/Mo(1 nm)/Ta(5 nm)/Ru(8 nm) on a silicon wafer with 300 nm silicon dioxide layer (Fig.1e). Excluding MgO, which was grown by radio-frequency sputtering from a ceramic MgO target, all other layers were grown by direct current sputtering of stoichiometric targets, in which case the Co-Fe-B alloy composition was (at. % 20/60/20). MTJMSD fabrication consisted of i) photolithography on the substrate to define the bottom electrode dimensions; ii) deposition of the Ta(5 nm)/Ru(8 nm)/Ta(5 nm)/Mo(1 nm)/CoFeB(6 nm) bottom electrode; iii) lift-off; iv) optical lithography for the insulator and thin top electrode cavity perpendicular to the bottom electrode; v) deposition of MgO, top CoFeB ferromagnet and capping layers and vi) magnetic molecules' attachment to the top and bottom electrode through a self-assembly electrochemical process (fig 1(a,b)). The optical and atomic force microscopy (AFM) images in figure 1(c-d) represent one MTJMSD cross junction of about ≈20 μm^2 area fabricated. A more detailed description of the experimental fabrication methods have been described previously [15,17]

RESULTS AND DISCUSSION:

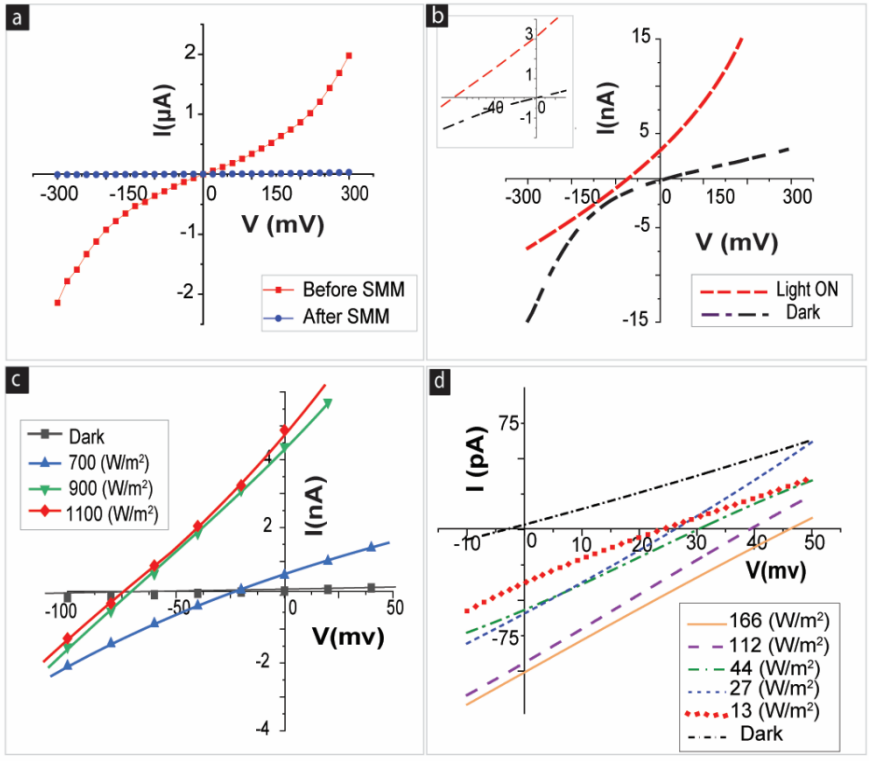

Figure 2: MTJMSD's cross junction IV measurement (a) before vs. after molecular treatment (b) in dark and light conditions (c) under different light intensities after two weeks (d) observing PV effect under various light intensities after 1.5 years.

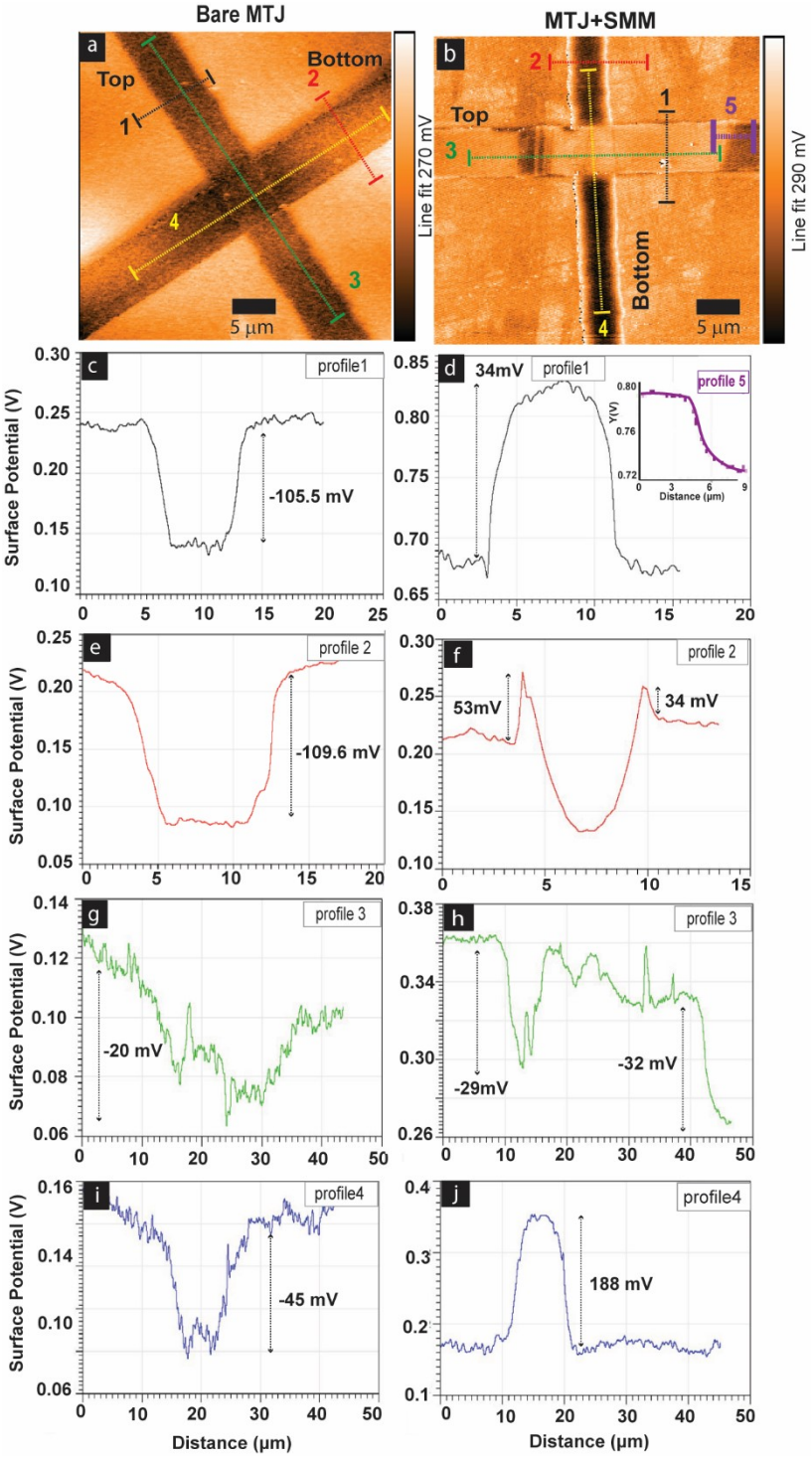

Figure 3: KPFM scan of MTJMSD's cross junction (a) before attaching molecules (b) after attaching molecule; (c-d) Surface potential of top electrode before Vs. after SMMs (e-f) Surface potential of bottom electrode before Vs. after SMMs; (g-h) difference between top and bottom electrode surface potential before and after SMM treatment along the length of electrodes; (i-j) difference between the top and bottom electrode before and after transforming bare MTJ into MTJMSD via molecule treatment

Figure 2a shows a current-voltage (IV) measurement of an MTJ before and after hosting SMM (Fig. 1c) molecular channels along the exposed sides to become MTJMSD (Fig. 1b). This transport study was performed under indoor ambient unfiltered light. We did not observe a noticeable effect of light on the bare tunnel junction transport across multiple studies (Fig. 2a), as indicated by the symmetric I-V characteristic that intersects zero voltage at zero current. However, following the formation of the SMM channel, two phenomena manifested themselves. MTJMSD settled into a suppressed current state, not observable in the scale used in Fig. 2a due to the nearly 1000-fold difference in current magnitude, and also started showing solar cell effect (Fig. 2b). In the dark, the MTJMSD current-voltage characteristic is analogous to that of a diode (Fig. 2b). Under ambient indoor light, the MTJMSD showed 3 nA saturation current and 80 mV open circuit voltage (Inset, Fig. 2b).

Since room light is different from actual sunlight, we studied MTJMSDs with a solar simulator (Solar Light®). The solar simulator's intensity was calibrated with Solar Light PMA 2100 Radiometer. We investigated the effect of variation in light intensity on the MTJMSD photovoltaic effect. We observed a large shift in open circuit voltage and saturation current as light intensity shifted from 700W/m^2 to 900 W/m^2 (Fig. 2c). Further increment in light intensity from 900 W/m^2 to 1100

W/m^2 did not yield significant change. We do not have a clear explanation to explain the impact of light intensity variation. However, in the prior work where another form of MTJMSD yielded a spin-photovoltaic effect, magnetic domains around the junction were varying over time[14,18]. We hypothesize that the rearrangement of magnetic ordering around the junction is associated with the impact of variation in the light intensity.

Our results show that the photovoltaic effect in MTJMSD's initial state under ≈100 W/m^2 (Fig. 2b) was comparable to the PV effect in two weeks aged MTJMSD under 700 W/m^2 (Fig. 2c). It is noteworthy that the 100 W/m^2 measurements were performed right after molecular treatment when MTJMSD had not reached to its equilibrium state yet. Also, there was a two weeks gap between the SMM treatment to form MTJMSD and arranging resources for the study with the solar simulator. Two weeks gap between SMM treatment and solar cell characterization (Fig. 2c) was believed to produce more ordered ferromagnetic electrodes. Temporal stabilization has been observed to produce different magnetic phases leading to various forms of the photovoltaic effect in the previous study by our group [14]. In our prior studies, the reason for spin photovoltaic effect[14] and long-range magnetic ordering around the junction area[18] was associated with the molecule-induced strong antiferromagnetic coupling[19].

We observe the prolonged aging effect in the MTMSD photovoltaic response by restudying the sample after 1.5 years. For this study, a variable-intensity light illuminator was utilized. The reason for using a low-intensity light source was to avoid any significant heating effect due to high-intensity solar simulator light radiation on the magnetic ordering of the aged sample. It must be noted that calibration of the light source is not critical in this study as we are unable to efficiency calculation. Light sources are basically used to check if photoresponse exists mainly due to light energy. For this study, we conducted transport measurements in dark and light after 1.5 year of SMM treatment of the MTJ. We observed that MTJ transport settled into a more suppressed current state in the pA range and junction responded to light exposure (Fig. 2d). In general, increasing white light intensity increased the photocurrent and open circuit voltage (Fig. 2d). However, roughly comparing the photoresponse in figure 2b on the freshly prepared MTJMSD vs. 1.5-year-old MTJMSD for roughly same light intensity the power production is more than two orders of magnitude smaller. Further studies are in order to monitor the evolution of magnetic phases and correlated photovoltaic effect as a function of time.

We also considered the possibility of the MTJMSD bottom electrode becoming oxidized during the fabrication state and subsequently aging with time. According to the literature, oxidized metals such as Cu_2O, WO_x, and FeO can produce the photovoltaic effect and have been used in forming complete solar cells [11,20,21]. Oxidized metals' optical properties, such as light reflection scattering and absorption, can vary significantly from their bare metal counterparts [22,23]. Our second photolithography step consists of coating the bottom electrode with photoresist and then curing the photoresist at 90 °C. Baking of a photoresist-covered bottom electrode with a CoFeB layer on top could cause the CoFeB layer to oxidation and change the bottom electrode's electric and magnetic properties. To attempt to rule out that the observed P.V. effect is not due to oxidation at the baking step, we carried out a controlled study with a reflectometer (Supplementary material Figure S1). To do so, MTJ was deposited up to the CoFeB layer on the bottom electrode, exposed to various temperatures for 30 minutes, and cooled down to room temperature for optical measurement. In this way we were able to follow changes in the reflectance spectra of the CoFeB layer evolving with increasing temperature. If oxidation takes place, we would have anticipated a significant change in reflectance signal intensity after a certain annealing temperature. In contrast, our results showed that CoFeB optical characteristics remain intact between room temperature (R.T.) and 100 ℃, and major changes started to occur only at further elevated temperature values.

We hypothesized that strong molecule-induced exchange coupling has to create the necessary properties in the ferromagnetic electrodes to absorb sufficient solar radiation. Molecules in the

MTJMSD itself are in the 0.001 μm x 4 μm =0.004 μm^2 area. The molecule channel area around the two edges is nearly 10,000 times smaller than the approximately 20 μm^2 junction area. An estimate of power generation/unit area with the molecular channel area leads to an unrealistic situation. If the molecular junctions local area is included exclusively in the calculation, the power output would be estimated to reflect a 100 times gain above the power incident upon the junction. Instead, the photovoltaic effect must arise from the larger areas, including the entire cross-tunnel junction.

We postulated that if SMM produced a room temperature stable photovoltaic effect, then it must have created room temperature stable long-range impact that can be observed in microscopy. To gain an in-depth understanding, we conducted Kelvin Probe Force Microscopy (KPFM) on MTJMSD junctions before- and after molecular treatment. On the bare MTJ before SMM treatment, KPFM exhibits similar results for both the top and bottom electrodes (Fig. 3a). Interestingly, we observed a stark change in ferromagnetic electrodes' surface potential after SMM attachment at room temperature. We observed the appearance of multiple phases in the top electrode (Fig. 3b) that were absent in the bare state of MTJ (Fig. 3a). The appearance of multiple phases is expected to be a built-in potential presence around the junction area. In our recent research on the anisotropy effect, we have discussed the role of voltage-induced anisotropy producing multiple phases on MTJMSD's magnetic electrode [24]. Interestingly, unlike the top electrode, the bottom electrode exhibited a very stable surface potential over a long range (Fig. 3b). The bottom electrode stack Ta/Ru/Ta/Mo/CoFeB was significantly modified over a whole area of observation that was at least 10 times larger in extent than the cross junction area (Fig. 3b). Based on the experimentally observed long-range impact, particularly on the bottom electrode, we conclude that molecules exert an impact beyond the junction area where molecules bridge between the two electrodes (Fig. 1b and e). Hence, it is highly likely that the light active region is associated with the entire region of change seen within the ferromagnetic electrodes, not only the local region where molecules are chemically bonded to the two electrodes along the two sides of the MTJ. Our current conclusion from this KPFM is consistent with

MFM and KPFM study performed on MTJMSD involving MTJ with Co/NiFe/AlOx/NiFe configuration and OMC molecules [14]. It is noteworthy that OMC paramagnetic molecule [14] differs from the SMM used in this study (Fig.1c).

We further investigated the SMM impact by focusing on different parts of the MTJ and MTJMSD along the line profiles indicated in Figures 3a and b. Line profile 1 on bare MTJ shows that the top electrode surface potential is 105±9 mV lower than that of the substrate (Fig. 3c). Interestingly, the line profile-1 on MTJMSD (Fig. 3d) shows that the top electrode surface potential was (130 ± 17) mV higher than that of the substrate (Fig. 3d). The top electrode surface potential after the molecule treatment changed from -105 mV to +130 mV with respect to the substrate after molecule bridging. The molecule has produced an approximate 235 mV potential difference on the top electrode. Interestingly, line profile 5 on MTJMSD's top electrode exhibited different surface potential in the two phases (Inset Fig. 3d), and this difference was (32 ± 1) mV.

We further investigated the surface potential of the bottom electrode of MTJ (Line profile 2-Fig. 3a) and MTJMSD (Line profile 2 -Fig.3b). Surface potential along the line profile 2 on the bottom electrode was (110 ± 15) mV lower than the substrate (Fig. 3e). The potential surface profile on the bottom electrode before SMM treatment (Fig.3e) was similar to the analogous profile on top electrode before SMM treatment (Fig. 3c). The difference between top and bottom electrode difference was ≈5 mV. However, the potential profile on the bottom electrode of MTJMSD (Fig. 3f) was starkly different as compared to the potential surface profile of the bottom electrode before the SMM treatment (Fig. 3e). Along the line profile2 (Fig.3b), the bottom surface potential profile was different around the electrode edge as compared the center (Fig. 3f). Interestingly, bottom electrode surface potential near the edges was more than that of substrate's surface potential (Fig. 3f). Bottom electrode edge surface potential

was (34 ± 2) mV more than the substrate potential (Fig. 3f). However, the surface potential in the middle of the electrode was (29 ± 1) mV lower with respect to the substrate potential.

We also compared the difference between top and bottom electrode surface potential before and after SMM treatment along the length of electrodes to observe the variations. The line profile 3 on bare MTJ before the molecule is shown (Fig. 3g). There is an average change of 20 mV along the length (Fig.3 g), and 5 mV perturbation around the junction area was observed (Fig. 3g). However, line profile 3 along the MTJMSD top electrode showed major perturbations at the sites of phase changes (Fig. 3h). The local perturbation at the site of left phase change was 29 mV, and right side of the phase change was 32 mV (Fig. 3h). To estimate the difference between the top and bottom electrode before and after transforming bare MTJ into MTJMSD via molecule treatment we studied on line profile 4 (Fig. i-j). The difference between the top and bottom electrodes before SMM treatment along the line4 profile was (45 ± 4) mV; the top electrode potential was lower than the bottom electrode (Fig. 3i). However, the difference between top and bottom electrodes after SMM treatment along the line4 profile was (188 ± 10) mV. It is remarkable the molecule bridging along the edges has resulted in an increase in potential difference from -45 mV to ≈188 mV, which amounts to approximately 230 mV. Based on our prior knowledge of the related device, the long-range impact on electrode potential is associated with the molecule-induced strong antiferromagnetic coupling, which in turn leads to the dramatic change in the spin density of states. Unfortunately, the current device structure with a nonmagnetic layer and very thin magnetic layers was difficult to study by other spectroscopies like MFM.

It is noteworthy that built-in potential generation in conventional p-n junction solar cells is directly associated with the difference in contact potential of the p and n regions [25,26]. We hypothesized that SMM's ability to produce a room-temperature stable large difference in contact potential between the top and the bottom electrode is producing an analogous built-in potential. However, unlike p-n junction solar cells where doping concentration yields the built-in potential, MTJMSD's built-in potential is solely due to the interaction of molecule spin with the two ferromagnetic electrodes. We also demonstrated previously that molecule-affected ferromagnetic electrodes in the MTJMSD junction area were able to absorb the light radiation [14]. We surmise that SMM-produced room temperature stable phases are light sensitive and, similar to semiconductors, have an energy gap. However, we are unable to provide an exact estimation of the energy gap between spin-related conduction and spin-related valance bands due to limited resources and complexity in MTJMSD geometry. Since light absorption and built-in potential in an MTJMSD is due to the spin interactions of SMM molecules and magnetic electrode, we termed MTJMSD's photovoltaic effect as the spin photovoltaic effect.

CONCLUSION: Magnetic tunnel junction-based molecular spintronics devices (MTJMSD) can be used as a testbed for a spin-current generation. We observed that a CoFeB/MgO/CoFeB based-MTJMSD shows a photovoltaic effect after single-molecule magnets (SMM) attachment along the exposed side edges. About 50% of our device junctions showed a photovoltaic effect under regular white light. However, open circuit voltage and saturation current changed over a period of one and a half years. According to our theoretical simulation, MTJMSD keeps stabilizing with time, and freshly made MTJMSD's magnetic properties differ from that after a long time. KPAFM has provided unique insights and suggests the contact potential on MTJMSD is a strong function of magnetic tunnel junction's ferromagnetic electrodes' properties. SMM used in this study did not produce any photovoltaic effect on nickel electrodes. Our KPAFM study also showed that the contact potential on the two electrodes of the MTJMSD was opposite and suggested the presence of a built-in potential causing the separation of photo-generated electrons in molecule impacted electrode. This work is consistent with the spin-photovoltaic effect observed on Co/NiFe/AlOx/NiFe and organometallic molecular cluster (OMC) based MTJMSDs. Future studies will focus on attempting different types of MTJ with a wide range of magnetic electrodes and molecule combinations to understand the exact mechanism and optimize solar cell

performance. We were unable to estimate efficiency because of the lack of knowledge about the area involved in solar electricity generation, which will be the focus of future work. The most exciting outcome of this research is that one can use earth-abundant Co, Fe, and Ni-like ferromagnetic materials for electricity generation. This work provides motivation for collaboration between MTJ researchers and chemists to explore the spin-photovoltaic and vast range of novel phenomena that can only be observed via the MTJMSD method. In summary, the pivotal factor in observing the spin photovoltaic effect is the SMM's ability to form spin channels between the two different ferromagnetic electrodes of an MTJ. The strong SMM-induced coupling catalyzes the long-range transformation of the electrode around the junction area. Notably, bare MTJ without SMM treatment did not produce a photovoltaic response under white light. Further advancements are possible by increasing the exchange coupling strength between ferromagnetic electrodes by using the short molecules, as compared to the approximately 3 nm long SMM used in this paper. We have produced a new MTJMSD scheme that allows the utilization of short molecules irrespective of the insulator's physical spacer thickness[27,28]. The major limitation of the current work discussed in this paper is that the insulator thickness must be smaller than the SMM length. Due to that limitation approach discussed here may not be suitable for large-area robust solar cell manufacturing using spin photovoltaic phenomenon.

Supplementary Information: Supplementary Information-ACS-Reflectance Spectra

ACKNOWLEDGMENTS:

We gratefully acknowledge the funding support, which was in part supported by the National Science Foundation-CREST Award (Contract No. HRD-1914751), Department of Energy/National Nuclear Security Agency (DE-FOA-0003945). This research was also funded by the Spanish Ministry of Science and Innovation [Grant numbers PID2019-109735GB-I00 and CEX2019-000919-M (Excellence Unit "María de Maeztu")] and Generalitat Valenciana [Grant number AICO/2021/295]. M.S. conducted experiments under the supervision of P.T. and D.G. P.S. did control experiments. CRD and JML synthesized the molecules. P.T. and M.S. wrote the manuscript that was edited by all the coauthors. We also appreciate support of NIST Gaithersburg's Center for Nanotechnology Science and Technology(CNST) award number N12.0057.01.

Competing interests

The authors have no relevant financial or non-financial interests to disclose.

Availability of data and material

Data used in this paper is available upon request.

Ethical Compliance: There is no human subject involvement.

REFERENCES:

1) Hirohata, A.; Yamada, K.; Nakatani, Y.; Prejbeanu, I.-L.; Diény, B.; Pirro, P.; Hillebrands, B.;*Review on spintronics: Principles and device applications*. *Journal of Magnetism and Magnetic Materials* **2020**, *509*, 166711.

2) Sun, X.; Vélez, S.; Atxabal, A.; Bedoya-Pinto, A.; Parui, S.; Zhu, X.; Llopis, R.; Casanova, F.; Hueso, L. E.;*A molecular spin-photovoltaic device*. *Science* **2017**, *357*, 677.

3) Wang, J.; Lu, H.; Pan, X.; Xu, J.; Liu, H.; Liu, X.; Khanal, D. R.; Toney, M. F.; Beard, M. C.; Vardeny, Z. V.;*Spin-Dependent Photovoltaic and Photogalvanic Responses of Optoelectronic Devices Based on Chiral Two-Dimensional Hybrid Organic–Inorganic Perovskites*. *ACS Nano* **2021**, *15*, 588.

4) Xu, H.; Wang, H.; Zhou, J.; Li, J.;*Pure spin photocurrent in non-centrosymmetric crystals: bulk spin photovoltaic effect*. *Nature Communications* **2021**, *12*, 4330.
5) Fabian, J.;*Spin-voltaic effect and its implications*. *Materials Transactions* **2003**, *44*, 2062.
6) Endres, B.; Ciorga, M.; Schmid, M.; Utz, M.; Bougeard, D.; Weiss, D.; Bayreuther, G.; Back, C.;*Demonstration of the spin solar cell and spin photodiode effect*. *Nature communications* **2013**, *4*, 2068.
7) Kondo, T.; Hayafuji, J.-j.; Munekata, H.;*Investigation of spin voltaic effect in ap–n heterojunction*. *Japanese journal of applied physics* **2006**, *45*, L663.
8) Hekking, F.; Nazarov, Y. V.;*Photovoltaic effect in quantum adiabatic transport as a way to pump electrons*. *Physical Review B* **1991**, *44*, 11506.
9) Pershin, Y. V.; Piermarocchi, C.;*Photovoltaic effect in bent quantum wires in the ballistic transport regime*. *Physical Review B* **2005**, *72*, 195340.
10) Fedorov, A.; Pershin, Y. V.; Piermarocchi, C.;*Spin-photovoltaic effect in quantum wires due to intersubband transitions*. *Physical Review B* **2005**, *72*, 245327.
11) Fedichkin, L.; Ryzhii, V.; V'yurkov, V.;*The photovoltaic effect in non-uniform quantum wires*. *Journal of Physics: Condensed Matter* **1993**, *5*, 6091.
12) Bottegoni, F.; Celebrano, M.; Bollani, M.; Biagioni, P.; Isella, G.; Ciccacci, F.; Finazzi, M.;*Spin voltage generation through optical excitation of complementary spin populations*. *Nature materials* **2014**, *13*, 790.
13) Sun, X. N.; Velez, S.; Atxabal, A.; Bedoya-Pinto, A.; Parui, S.; Zhu, X. W.; Llopis, R.; Casanova, F.; Hueso, L. E.;*A molecular spin-photovoltaic device*. *Science* **2017**, *357*, 677.
14) Tyagi, P.; Riso, C.;*Molecular spintronics devices exhibiting properties of a solar cell*. *Nanotechnology* **2019**, *30*, 495401.
15) Tyagi, P.; Riso, C.; Friebe, E.;*Magnetic Tunnel Junction Based Molecular Spintronics Devices Exhibiting Current Suppression At Room Temperature*. *Organic Electronics* **2019**, *64*, 188.
16) Li, D. F.; Parkin, S.; Wang, G. B.; Yee, G. T.; Clerac, R.; Wernsdorfer, W.; Holmes, S. M.;*An S=6 cyanide-bridged octanuclear (Fe4Ni4II)-Ni-III complex that exhibits slow relaxation of the magnetization*. *J. Am. Chem. Soc.* **2006**, *128*, 4214.
17) Tyagi, P.; Riso, C.; Amir, U.; Rojas-Dotti, C.; Martínez-Lillo, J.;*Exploring room-temperature transport of single-molecule magnet-based molecular spintronics devices using the magnetic tunnel junction as a device platform*. *RSC Advances* **2020**, *10*, 13006.
18) Tyagi, P.; Riso, C.;*Magnetic force microscopy revealing long range molecule impact on magnetic tunnel junction based molecular spintronics devices*. *Organic Electronics* **2019**, *75*, 105421.
19) Tyagi, P.; Baker, C.; D'Angelo, C.;*Paramagnetic Molecule Induced Strong Antiferromagnetic Exchange Coupling on a Magnetic Tunnel Junction Based Molecular Spintronics Device*. *Nanotechnology* **2015**, *26*, 305602.
20) Tran, T. A.; Trinh, T. T.; Viet, T. D.; Do, H. B.; Giang, N. T. T.; Kim, S.; Pham, D. P.; Yi, J.; Dao, V.-A.;*Effects of oxidation state on photovoltaic properties of reactively magnetron sputtered hole-selective WOx contacts in silicon heterojunction solar cells*. *Semiconductor Science and Technology* **2020**, *35*, 045020.
21) Ameur, A.; Berrada, A.; Loudiyi, K.; Adomatis, R. In *Hybrid Energy System Models*; Elsevier: 2021, p 195.
22) Leberknight, C. E.; Lustman, B.;*An Optical Investigation of Oxide Films on Metals*. *J. Opt. Soc. Am.* **1939**, *29*, 59.
23) Blewett, D. T.; Cahill, J. T.; Lawrence, S. J.; Denevi, B. W.; Nguyen, N. V. 2012; Vol. 2012, p P12A.
24) Dahal, B. R.; Savadkoohi, M.; Grizzle, A.; D'Angelo, C.; Lamberti, V.; Tyagi, P.;*Easy axis anisotropy creating high contrast magnetic zones on magnetic tunnel junctions based molecular spintronics devices (MTJMSD)*. *Scientific reports* **2022**, *12*, 1.

25) Kittel, C. *Intorduction to Solid State Physics*; 7th ed.; John Wiley & Sons, Inc: New York, 1996.
26) Polak, L.; Wijngaarden, R. J.;*Two competing interpretations of Kelvin probe force microscopy on semiconductors put to test*. *Physical Review B* **2016**, *93*, 195320.
27) Tyagi, P.; USPTO, Ed. USA, 2023, p U.S. Patent Application No. US17/033.
28) Tyagi, P.; USPTO, Ed. 2020, p U.S. Patent Application No. 16/102.